

See discussions, stats, and author profiles for this publication at: <https://www.researchgate.net/publication/51730014>

Polymorphism and Mesomorphism of Oligomeric Surfactants: Effect of the Degree of Oligomerization

ARTICLE in LANGMUIR · DECEMBER 2011

Impact Factor: 4.46 · DOI: 10.1021/la203777c · Source: PubMed

CITATIONS

8

READS

26

5 AUTHORS, INCLUDING:



Darija Jurašin

Ruđer Bošković Institute

24 PUBLICATIONS 127 CITATIONS

[SEE PROFILE](#)



Andjela Pustak

Ruđer Bošković Institute

14 PUBLICATIONS 67 CITATIONS

[SEE PROFILE](#)



Ivan Šmit

Ruđer Bošković Institute

72 PUBLICATIONS 1,011 CITATIONS

[SEE PROFILE](#)



Nada Filipović-Vinceković

Ruđer Bošković Institute

95 PUBLICATIONS 963 CITATIONS

[SEE PROFILE](#)

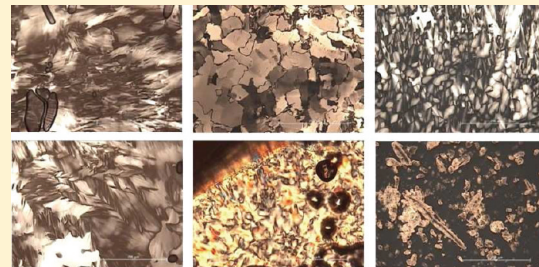
Polymorphism and Mesomorphism of Oligomeric Surfactants: Effect of the Degree of Oligomerization

D. Jurašin,^{*,†} A. Pustak,[‡] I. Habuš,[†] I. Šmit,[‡] and N. Filipović-Vinceković[†]

[†]Division of Physical Chemistry and [‡]Division of Materials Chemistry, Ruđer Bošković Institute, Zagreb, Bijenička cesta 54, Croatia

 Supporting Information

ABSTRACT: A series of cationic oligomeric surfactants (quaternary dodecyldimethylammonium ions with two, three, or four chains connected by an ethylene spacer at the headgroup level, abbreviated as dimer, trimer, and tetramer) were synthesized and characterized. The influence of the degree of oligomerization on their polymorphic and mesomorphic properties was investigated by means of X-ray diffraction, polarizing optical microscopy, thermogravimetry, and differential scanning calorimetry. All compounds display layered arrangements with interdigitated dodecyl chains. The increase in the degree of oligomerization increases the interlayer distance and decreases the ordering in the solid phase; whereas the dimer sample is fully crystalline with well-developed 3D ordering and the trimer and tetramer crystallize as highly ordered crystal smectic phases. The number of thermal phase transitions and sequence of phases are markedly affected by the number of dodecyl chains. Anhydrous samples exhibit polymorphism and thermotropic mesomorphism of the smectic type, with the exception of the tetramer that displays only transitions at higher temperature associated with decomposition and melting. All hydrated compounds form lyotropic mesophases showing reversible phase transitions upon heating and cooling. The sequence of liquid-crystalline phases for the dimer, typical of concentrated ionic surfactant systems, comprises a hexagonal phase at lower temperatures and a smectic phase at higher temperatures. In contrast, the trimer and tetramer reveal textures of the hexagonal phase.



INTRODUCTION

Oligomeric surfactants are a wide class of amphiphilic molecules consisting of two to four monomeric surfactant moieties coupled by spacer groups at the level of (or very close to) headgroups. These surfactants represent a transient group of surfactants between monomeric and polymeric ones, showing remarkably different solution and interfacial behavior from their monomeric analogues.¹ The presence of spacer groups and the degree of oligomerization allow the synthesis of oligomers of an enormous variety of structures with various solution properties.^{2–4} At present, most of the research on oligomeric surfactants focuses on their self-association in solution and adsorption at interfaces. In spite of numerous papers dealing with solution and interfacial properties of oligomeric surfactants, there are several reports on the structural and thermal behavior of gemini surfactants in their anhydrous state;^{2,5–13} however, there are hardly any reports in the literature on the structural and thermal behavior of anhydrous quaternary ammonium bromide surfactants with three or four alkyl chains connected at the level of headgroups by a short spacer.

We have recently described the synthesis and influence of the degree of oligomerization on aggregation in solution and adsorption at the air/solution interface of a series of oligomeric quaternary ammonium bromide surfactants containing dodecyl chains connected by an ethylene spacer at the headgroup level (abbreviated as 12-2-(12-2)_x-12, where *x* denotes the degree of oligomerization having values of 0, 1, or 2).¹⁴ It was shown that both adsorption and aggregation strongly depend on the number

of hydrophobic tails and on the bimodal charge distribution of ionic headgroups at both the air/solution and micelle/solution interfaces. In this article, we report the polymorphic and mesomorphic (both thermotropic and lyotropic) behavior of oligomeric surfactants as well as their corresponding monomeric compound dodecyltrimethylammonium bromide. It will be shown that, in comparison with their monomeric counterpart, oligomeric surfactants exhibit peculiar structural and thermal properties.

EXPERIMENTAL SECTION

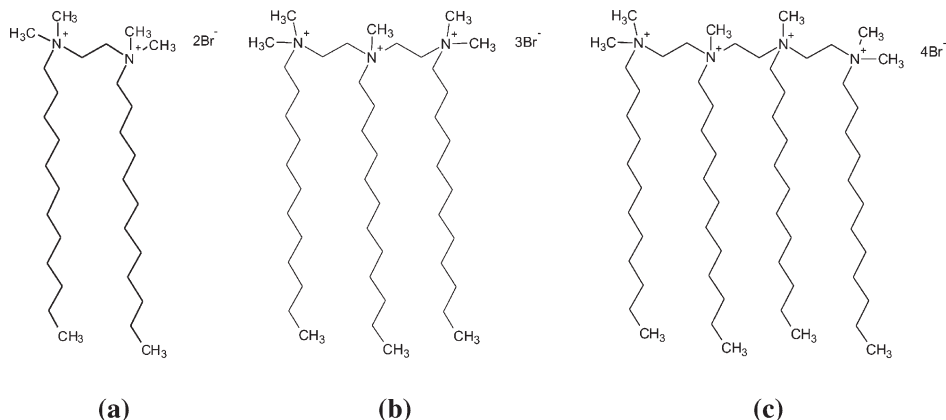
Materials. Dodecyltrimethylammonium bromide (denoted as DTAB) was commercially obtained (Fluka, Germany) and recrystallized from acetone. A series of cationic oligomeric surfactants in which *n*-dodecyltrimethylammonium chains were connected at polar headgroups by an ethylene spacer have been synthesized. Oligomeric surfactants with two, three, and four dodecyl chains (i.e., bis(*N,N*-dimethyl-*N*-dodecyl)ethylene-1,2-diammonium dibromide, bis [2-(*N',N'*-dimethyl-*N*'-dodecylammonio)ethylene]-*N*-dodecyl-*N*-methylammonium tribromide, and *N,N'*-bis[2'-(*N'',N''*-dimethyl-*N''*-dodecylammonio)ethylene]-*N*,*N*'-didodecyl-*N',N'*-dimethyl-ethylene-1,2-diammonium tetrabromide) are denoted as 12-2-12 (Scheme 1a), 12-2-12-2-12 (Scheme 1b), and

Received: September 27, 2011

Revised: October 19, 2011

Published: October 19, 2011

Scheme 1. Chemical Structures of 12-2-(12-2)_x-12 Surfactants



12-2-12-2-12-2-12 (Scheme 1c) or only as dimer, trimer, and tetramer, respectively.

The dimer was prepared in refluxing acetonitrile as described by Imam et al.¹⁵ The trimer and tetramer were prepared and characterized as described previously.¹⁴ Reaction mixtures of 1-dodecylbromide with *N,N,N',N'',N'''-pentamethyldiethylenetriamine* or *N,N,N',N'',N'',N'''-hexamethyltriethylenetetramine* in DMF were held at 80 °C for 144 h and at 100 °C for 192 h. Reactions were performed in a dry, inert atmosphere of argon in reaction vials (total capacity 50 mL, closed with screw caps and silicone septa) under pressures created by the temperatures in closed reaction systems. IR and ¹H NMR spectra as well as elemental analyses and the absence of minima surface tension isotherms confirmed the high purity of the prepared compounds.¹⁴

Melting Point. Melting points were determined on a Reichert Thermovar 7905 apparatus and were not corrected.

Thermogravimetric Analysis (TGA). Thermogravimetry was performed from 20 to 400 °C with a Mettler TA 4000 system.

Differential Scanning Calorimetry (DSC). Thermal phase transitions were detected by differential scanning calorimetry (Perkin-Elmer DSC7 calorimeter). Samples were heated from ambient temperature at a rate of $5\text{ }^{\circ}\text{C min}^{-1}$. Transition temperatures were reported as the maxima and minima of their endothermic and exothermic peaks. The solid sample for DSC analysis was put into an aluminum capsule and heated. The enthalpy of the phase transition (ΔH) was determined from the peak area of the DSC curve. The corresponding transition entropy value (ΔS) was calculated from the equation $\Delta S = \Delta H/T$, where T is the transition temperature corresponding to the DSC maximum. Data presented in the results are mean values of several independent measurements on different samples, with the standard deviation being $\pm 5\%$.

Microscopic Observations (POM). The morphology and textures of solid phases were observed with a light-polarizing microscope (Leica DM LS) equipped with a Mettler FP 82 hot stage, a camera, and a scanning electron microscope (Phillip's XL30). Hydrated solids were prepared directly between a microscope slide and a coverslip by placing a drop of water on a layer of surfactant (the sample concentration was 95%), which was slowly heated. The mesophases were identified by comparing their texture to photomicrographs from the literature.¹⁶

X-ray Diffraction (XRD). An automatic X-ray powder diffractometer having a high-temperature attachment (Philips MPD 1880; monochromatic Cu $K\alpha$ radiation, proportional counter) was used for analysis at room temperature (recorded in the region of $2\theta/^\circ = 3-50$) and higher temperatures (recorded in the region of $2\theta/^\circ = 5-35$) in the Bragg angle region. Temperatures for recorded high-temperature XRD were chosen between the points of phase transitions, in accordance with

the DSC curves. During the heating runs, heating was stopped at a chosen temperature for 20 min in order to take diffraction patterns. The interlayer spacing (d_{hkl}) was calculated according to Bragg's law.¹⁷

■ RESULTS AND DISCUSSION

Structural Properties of Anhydrous Surfactants. Structural information on the phase type of surfactant samples was obtained by powder X-ray diffraction studies at room temperature. Figure 1a–d represents the X-ray diffraction patterns of 12-2-(12-2)_x-12 surfactants and their monomer analogue DTAB with indexed characteristic reflections. All diffractograms show small-angle reflections with reciprocal spacing in the ratio 1:2:3:4, indicating that the molecules are ordered in layers. The major repeat distances (interlayer distances) were calculated from the repeating 00l reflections for all samples.

Diffraction patterns of DTAB and the dimer with a number of sharp Bragg reflections without amorphous halos show the existence of fully crystalline samples with well-developed 3D ordering. The crystal properties and molecular packing of DTAB and the dimer have already been determined.^{18,19} DTAB crystallizes in monoclinic space group $P2_1$,¹⁸ and the dimer crystallizes in space group $P\bar{1}$ with lower triclinic symmetry.¹⁹ In contrast, the diffraction patterns of the trimer and tetramer exhibit one strong sharp reflection in the small-angle region and several rather broadened ones superimposed on amorphous maxima. Such diffraction patterns indicate the existence of less-ordered solid phases, and their structures were not determined.

The major repeat distance of DTAB ($d_{001} = 21.25 \text{ \AA}$) determined from the first reflection is comparable to the dimension of the unit cell c axis (21.55 Å).¹⁸ Considering the dimensions of two extended dodecyl chains in the trans configuration ($2 \times 16.7 \text{ \AA} = 33.4 \text{ \AA}$),²⁰ the shortest distance of the ionic headgroup from the α -carbon atom (1.80 Å),^{21a} and the ionic radii of the trimethylammonium group (2.94 Å)^{21b} and the bromide ion (1.13 Å),^{21b} the calculated value of the interplanar spacing is much higher than experimentally determined. It indicates a head-to-tail arrangement within each layer, that is, the interdigitation of dodecyl chains.

The connection of two monomers with charged quaternary centers by an ethylene spacer in a molecule of 12-2-12 decreases d_{001} compared to DTAB. Polar headgroups $\text{N}(\text{CH}_2)(\text{CH}_3)_2^+$ adopt a chiral conformation in the solid state.¹⁹ Accordingly, the

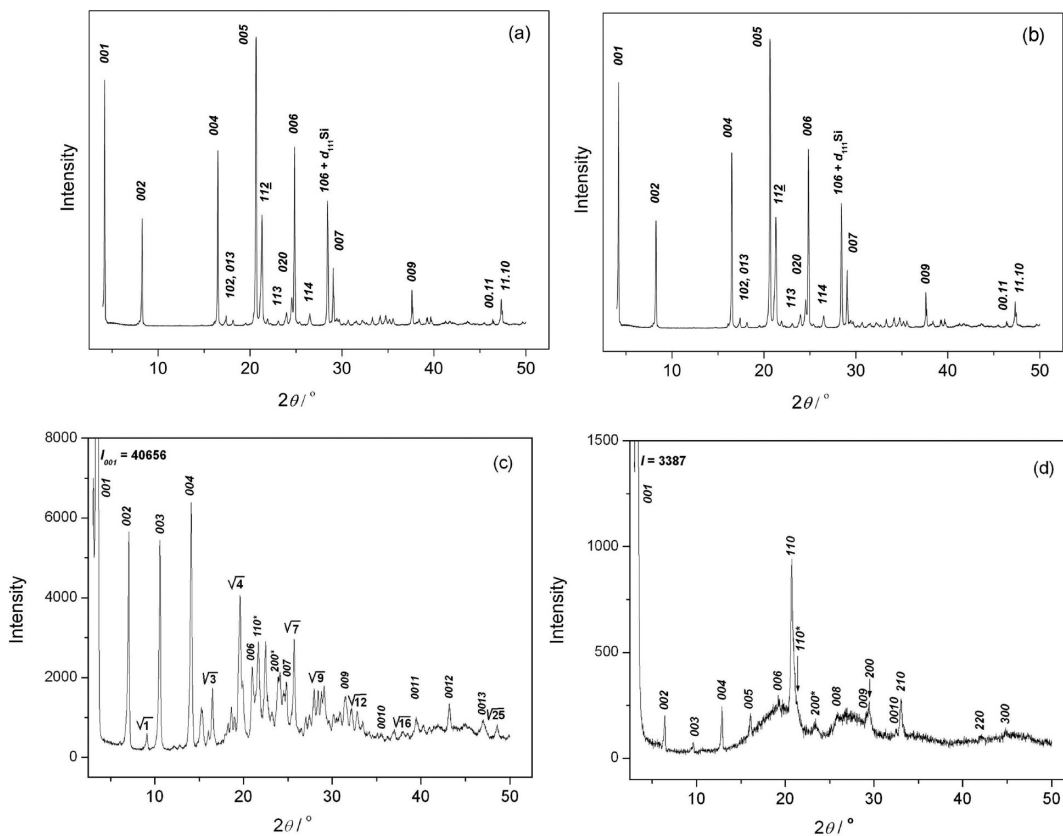


Figure 1. X-ray diffraction patterns of DTAB (a), 12-2-12 (b), 12-2-12-2-12 (c), and 12-2-12-2-12-2-12 (d) taken at room temperature.

12-2-12 surfactant crystallizes with dodecyl chains in a trans conformation with respect to the spacer plane ($\text{N}^+-(\text{CH}_2)_2-\text{N}^+$), similarly to those observed in the crystal of 4-2-4.⁹ The major periodicity $d_{001} = 15.48 \text{ \AA}$, repeated up to the sixth-order reflection, corresponds to the c axis of the triclinic unit cell (15.74 \AA^{19}). Hydrocarbon chains aligned in the direction of the long axis are set side by side in a tail-to-tail configuration (Figure 2a–c). Accordingly, the dimension of two extended dodecyl chains in the trans configuration is even more than twice as large as the interplanar spacing d_{001} , indicating that two crystallographic cells comprise more than one molecule in the trans conformation.

To obtain broader information, the diffraction pattern of the 12-2-12-2-12 sample aged several months at room temperature is presented in Figure 1c instead of the freshly prepared sample that exhibited hexagonal mesomorphic ordering (Figure 7c). Significantly sharper $00l$ reflections in the diffractogram of the aged anhydrous sample compared to those in the diffractogram of the freshly prepared anhydrous sample indicate better interlayer stacking. Aging at room temperature acts as an annealing process (e.g., the ordering of the cast trimer sample is kinetically influenced). The diffraction pattern in Figure 1c shows multiple sharp reflections at small and medium angles with the first four $00l$ reflections being very strong. The layer periodicity calculated from the first extraordinary strong peak is $d_{001} = 25.07 \text{ \AA}$. Sharp reflections superimposed on two diffuse amorphous maxima indexed with a ratio of $1:(3)^{1/2}:(4)^{1/2}:(7)^{1/2}:(9)^{1/2}:(12)^{1/2}:(16)^{1/2}:(25)^{1/2}$ of reciprocal spacings indicate the lateral hexagonal arrangement of ammonium headgroups and bromide counterions within smectic layers. Unit cell parameter a in the hexagonal lattice calculated from the interplanar d_{100} value

indexed as 1 in Figure 1c (which usually follows reflection 002) is 11.32 \AA . Reflections centered at ca. 4.10 \AA and 3.72 \AA and indexed as reflections 110 and 200 of a 2D centered rectangular lattice (denoted as 110^* and 200^*) correspond to the lateral ordering of alkyl chains within the smectic layers.^{22,23} A few other hkl diffraction lines indicating advanced ordering are an obstacle to indexing and a more detailed interpretation of patterns. They might also be pseudo-Bragg peaks superimposed on amorphous halos (indicating disorder) by which crystal mesophases (actually crystal B phases) were distinguished from crystals.¹⁶ Namely, highly ordered smectic phases are no longer considered to be true liquid-crystalline phases because they are no longer regarded as true smectic phases. They are denoted by a letter code that refers to their smectic liquid-crystalline phase but without their smectic code letter Sm.²² Accordingly, the trimer can be denoted as a crystal smectic B phase. In the crystal smectic B phase, like the hexatic B and smectic A phases, the molecules are arranged in layers with their long axes orthogonal to the layer planes. The main difference between the crystal smectic B phase and the hexatic B phase is that the molecules in the crystal smectic B phase have long-range positional order but also exhibit rapid dynamic motion. This makes the phase similar to a plastic crystal; therefore, the crystal smectic B phase could be called an anisotropic soft crystal.¹⁶

Relatively narrow reflections of tetramer powder, superimposed on four diffuse amorphous maxima, apparently indicate only a semicrystalline specimen (Figure 1d). A very intensive first reflection at a small diffraction angle and a characteristic ratio of reciprocal spacing values of $1:2:3:4:5:6:7:8:9:10$ undoubtedly indicate layered ordering with a layer distance of $d_{001} = 27.25 \text{ \AA}$.

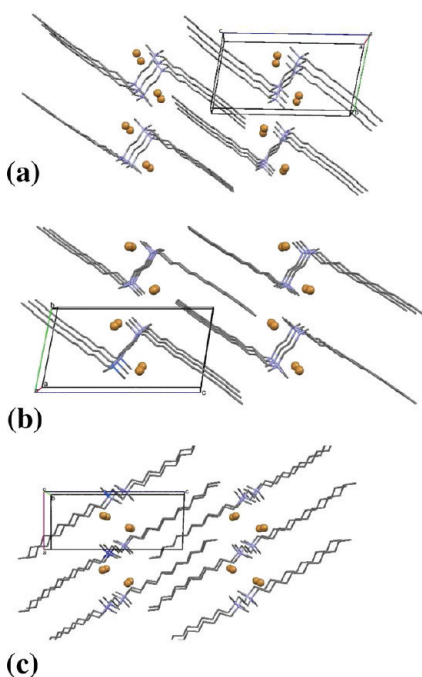


Figure 2. Stereoscopic view of dimer molecules with the unit cell (a) and arrangement of dimer molecules viewed along the *a* (b) and *b* axes (c) constructed according to ref 19. Alkyl chains are in black, ammonium groups are in blue, and bromides are in brown. The *a* axis is red, the *b* axis is green, and the *c* axis is blue.

A strong reflection at 4.26 Å and weaker reflections at 3.02 and 2.74 Å with reciprocal spacing in the ratio (2)^{1/2}:(4)^{1/2}:(5)^{1/2} (of planes 110/200/210) are indicative of the tetragonal arrangement of ammonium headgroups and bromide counterions within smectic layers. The peaks at 3.02 and 2.70 Å seem to be combined from two reflections, 009 + 200 (centered at 3.02 Å) and 0010 + 210 (centered at 2.74 and 2.70 Å), respectively. The lateral packing of ionic species within alkyl chain layers could be ascribed to a smectic mesophase with 2D tetragonal symmetry. This mesophase with the lateral tetragonal ordering of stable ions in sublayers (which interrupts 3D ordering in the longitudinal direction) is named in accord with a new type of ordered smectic mesophase, the smectic T phase,²⁴ and a crystal smectic T phase.²⁵ Unit cell parameter *a* of the square lattice (for a 2D square lattice, $1/d_{hk}^2 = (h^2 + k^2)/a^2$) calculated from 110, 200, 210, and 300 reflections is *a* = 6.04 Å. Weak reflections, centered at ca. 4.16 and 3.78 Å, are indexed as 110 and 200 reflections of a 2D-centered rectangular lattice (i.e., 110* and 200*) and correspond to the partial lateral ordering of alkyl chains within the smectic layers. However, low intensities of these reflections beside the significant amorphous halo at *d* = 4.42 Å indicate that most of the alkyl chains are in a disordered state.

Obviously, ammonium headgroups and bromide counterions simultaneously maintain a longitudinal smectic order (00*l* reflections) and a mesomorphic lateral tetragonal order (other reflections) in the tetramer. The diffractogram of the tetramer exhibits four diffuse diffraction halos with peak intensities of around $2\theta/\circ = 20.1$ (*d* = 4.42 Å), 28.2 (*d* = 3.16 Å), 35.9 (*d* = 2.50 Å), and 46.6 (*d* = 1.95 Å) in comparison with paraffin-based mesostructures containing mainly one diffuse halo at *d* ≈ 4.5 Å characteristic of the disordered liquidlike conformation of alkyl chains.²⁶ These halos may arise through diffraction from the

disordered liquidlike conformation of liquid paraffins (*d* = 4.42 Å) as well as from unsatisfactory interlayer stacking and the sublayer periodicity of ordered ammonium headgroups and bromide counterions.

Scanning electron microscopy images showing the stacking of layers at the edge of the crystals provide auxiliary evidence for the lamellar structure (Figure 3a–d).

Major factors influencing the oligomeric surfactant molecular packing in a crystal lattice are the electrostatic forces between ammonium headgroups and bromide counterions and the van der Waals interactions between the alkyl chains and hydrogen bonds.⁷ All forces contribute to the lattice energy, and their relative strengths determine the crystal structure. The forces in the ionic layer are very strong compared to the van der Waals forces in the hydrocarbon layer, causing the segregation of ionic and hydrophobic parts and packing in lamellar layers. The major interlayer distance increases from dimer to tetramer; however, all *d* values being significantly lower than for double extended dodecyl chains indicates chain interdigitation. Stacking together many layers forms a bulk crystalline phase. Similar observations of the lamellar type of layered structure are also found in sulfonic acid-doped thermoreversible polyaniline gels.^{27,28} Similarly to its monomeric counterpart, the dimer exhibits a diffraction pattern with a number of sharp Bragg reflections without an amorphous halo, showing the existence of a fully crystalline sample. Diffraction patterns of the trimer and tetramer are typical of highly ordered crystal smectic phases (crystal smectic B and T, respectively), which are considered to be anisotropic soft crystals. They differ from a true crystal phase in that their thermal motion is not completely frozen out (i.e., they have freedom of rotation about their long axes). When the degree of oligomerization increases, the ordering in the samples decreases. There is no doubt that this can be attributed to the geometric constraints imposed by the number of dodecyl chains and the extension of adjacent dodecyl chains on each side of the spacer plane.

Polymorphism and Thermotropic Mesomorphism of Anhydrous Surfactants. Thermally induced structural changes were studied by several methods that complement each other. The thermal stability of the compounds was assessed by TGA, and the data are shown in Table 1. All compounds start to decompose slowly as a function of the number of alkyl chains and do not show the presence of bound water.

Figure 4 presents the dependence of the melting point (*T*_{mp}) and temperature of maximum decomposition (*T*_{peak}) on the number of carbon atoms (*n*) in the investigated compounds. The *T*_{mp} of oligomeric surfactants increases linearly with the degree of oligomerization, and can be approximated by the equation $T_{mp} = 52.6 + 3.7n$. This is in accord with the well-known fact that the number of carbon atoms influences the different properties of hydrocarbons. Slow decomposition of DTAB and the dimer starts in the vicinity of *T*_{mp}, with *T*_{peak} well above the melting temperature. The peak decomposition temperature occurs for the trimer in the vicinity of its melting point and for the tetramer below its melting point. It can be seen that the temperature difference between the *T*_{mp} of the solid phase and *T*_{peak} drastically decreases with the degree of oligomerization.

The melting point of an organic compound depends on the strength of its crystal lattice, which is related to intermolecular forces. For ionic surfactants, close-packed headgroups and counterions produce strong electrostatic interactions, resulting in higher melting points. In spite of the increasing number of headgroups, the melting point of the dimer is slightly lower than

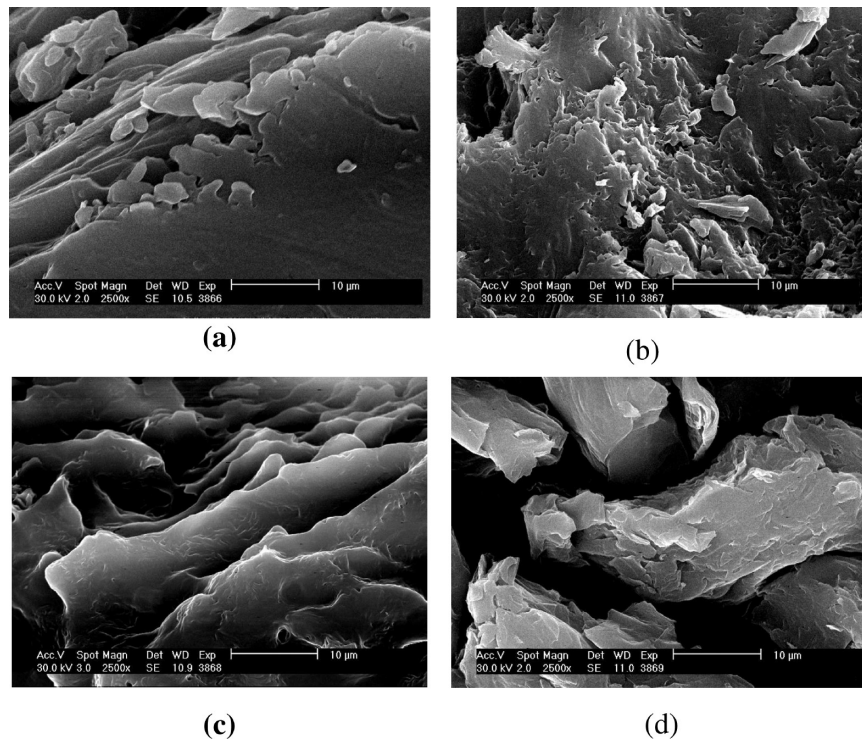


Figure 3. Scanning electron micrographs of DTAB (a), 12-2-12 (b), 12-2-12-2-12 (c), and 12-2-12-2-12-2-12 (d). Bars are indicated.

Table 1. Thermal Decomposition Data of the 12-2-(12-2)_x-12 Surfactants and Their Monomer Analogue DTAB^a

| compound | T _{start} /°C | T _{peak} /°C | T _{end} /°C | Δm/% |
|-------------------|------------------------|-----------------------|----------------------|--------|
| DTAB | 157.0 | 229.0 | 339.0 | 96.461 |
| 12-2-12 | 138.7 | 215.7 | 331.2 | 90.774 |
| 12-2-12-2-12 | 135.0 | 224.8 | 388.0 | 92.940 |
| 12-2-12-2-12-2-12 | 168.0 | 259.7 | 378.8 | 88.866 |

^a T is the temperature (starting, peak, and end) for the main steps, and Δm is the mass loss.

that of its monomeric counterpart. Besides the interaction between headgroups, the attractive forces between dodecyl tails also affect the melting point to a certain extent. Obviously, the interaction between dodecyl chains in DTAB is intensified in comparison with dodecyl chains in the dimer, which are in a trans conformation with respect to the short spacer.

DSC was used for the quantitative detection of phase transitions. Keeping in mind the thermal instability and partial decomposition of oligomeric surfactants, the results were taken from the first heating runs (repeated heating–cooling cycles could not be completed). Heating curves of DTAB, the dimer, and the trimer exhibit several distinct endothermic transitions depending on the number of dodecyl chains (Figure 5). The DSC heating curve of the tetramer revealed only one exothermic transition associated with decomposition and melting (not shown). The phase-transition parameters (maximum transition temperatures and changes in enthalpy and entropy derived from heating scans) for the investigated compounds are listed in Table 2.

At room temperature, all compounds appeared as a white powder showing anisotropy under crossed polarizers. DTAB

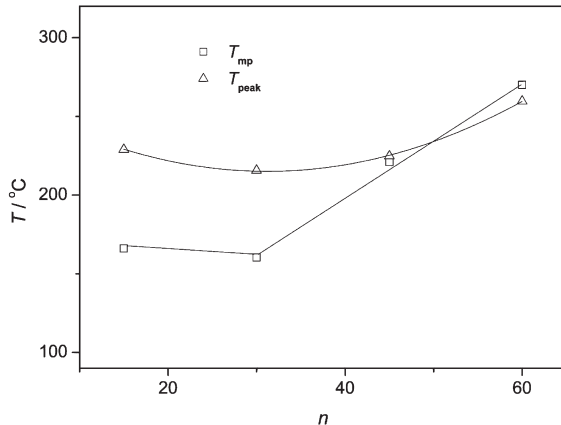


Figure 4. Changes in the melting point (T_{mp}) and temperature of maximum decomposition (T_{peak}) with the number of carbon atoms (n) in the 12-2-(12-2)_x-12 surfactants and their monomer analogue DTAB.

appeared as agglomerates of platelets (Figure 6a), dimer and trimer appeared as agglomerates of small, irregularly shaped crystals (Figure 1SI), and the tetramer appeared as a mixture of transparent lancetlike crystals and agglomerates of smaller particles (Figure 6g). Microscopic monitoring showed that melting coincided with the last transitions; an exception is the tetramer, which decomposed prior to melting (Figure 6h). This means that transitions at lower temperatures subsume structural changes inside the solid crystalline phase (SC) (i.e., a solid-to-solid transition). DTAB displayed two endothermic transitions below melting, the first of which was associated with a small enthalpy change and the second of which was associated with a large enthalpy change. X-ray analysis (Figure 7a) revealed that the first

phase transition corresponds to the formation of structural variety (SC_1^*) of the room-temperature phase (SC_1) and the second phase transition corresponds to polymorphic transition (SC_2). Examination under a polarizing microscope showed many wrinkles, softening, and the partial loss of anisotropy

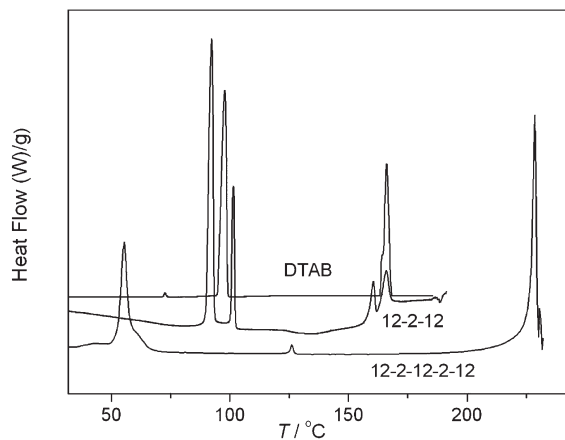


Figure 5. DSC heating curves of DTAB, 12-2-12, and 12-2-12-2-12.

Table 2. Transition Temperatures T (Corresponding to the DSC Maximum), Enthalpies (ΔH), and Entropies (ΔS) of the 12-2-(12-2)_x-12 Surfactants and Their Monomer Analogue DTAB at a Heating Rate of 5 °C min⁻¹

| compound | $T/^\circ\text{C}$ | $\Delta H/\text{kJ mol}^{-1}$ | $\Delta S/\text{J mol}^{-1} \text{K}^{-1}$ |
|-------------------|--------------------|-------------------------------|--|
| DTAB | 72.3 | 0.3 | 0.9 |
| | 97.5 | 39.8 | 107.3 |
| | 166.0 | 28.9 | 65.8 |
| 12-2-12 | 92.2 | 41.8 | 114.4 |
| | 101.4 | 8.6 | 23.0 |
| | 160.3 | 1.2 | 2.8 |
| | 166.0 | 1.3 | 3.0 |
| 12-2-12-2-12 | 55.5 | 31.6 | 96.2 |
| | 126.1 | 1.1 | 0.5 |
| | 228.6 | 54.9 | 109.4 |
| 12-2-12-2-12-2-12 | 273.7 | -9.6 | -17.5 |

after the second transition (Figure 6b). This might be explained by the existence of amorphous layers, which occupy a large part of the compound.²⁹ During melting, DTAB passed directly from the crystalline state into the isotropic liquid (IL) without an intermediate liquid-crystalline state (LC); that is, DTAB exhibited polymorphism but no mesomorphism. On heating, phase transitions can be represented by the sequence $SC_1 \rightarrow SC_1^* \rightarrow SC_2 \rightarrow IL$, where subscript 1 denotes the room-temperature phase and 1* and 2 denote higher-temperature phases. On cooling, the DSC curve showed two sharp exothermic peaks (Figure 2SI): one at 148 °C (transition from IL to SC_2) and the other at 80 °C (polymorphic transition from SC_2 to SC_1). Both phase transitions proceeded with temperature hysteresis without the appearance of the SC_1^* phase. Almost the same enthalpy and entropy changes for two main transitions during the heating and cooling cycles indicate the high stability of both polymorphs.

Two closely spaced endothermic transitions at lower temperatures of the dimer, associated with a relatively high enthalpy change, can be ascribed to two polymorphic transitions, whereas two closely spaced endothermic transitions at higher temperatures, associated with a small enthalpy change, are typical of the liquid-crystalline phase transitions. A “cloudy” birefringent texture similar to that of a viscous neat phase observed beyond the second transition indicates the transition from the crystal phase to the SmC phase (or L_β phase), as shown in Figure 7c and previously in the literature.^{2,6} Upon further heating, the SmC phase transformed into a viscous fluid with oily streak textures (Figure 6c) and Maltese crosses (Figure 6d), indicating the formation of the SmA phase. Thermal transitions for the dimer can be described as follows: $SC_1 \rightarrow SC_2 \rightarrow SmC \rightarrow SmA \rightarrow IL/decomposition$. Transition to the IL phase associated with the appearance of a small amount of black solid indicates decomposition during the LC-IL transition. On cooling from the IL phase, DSC curve showed only two exothermic transitions (Figure 2SI), both associated with a small enthalpy change (-6.1 and 0.2 kJ mol⁻¹). Differences between heating and cooling DSC data are indicative of the onset of decomposition.

On heating, the trimer exhibited two endothermic transitions below melting; the first is associated with a relatively high enthalpy change and the second is associated with small enthalpy changes. Softening of the material observed after the

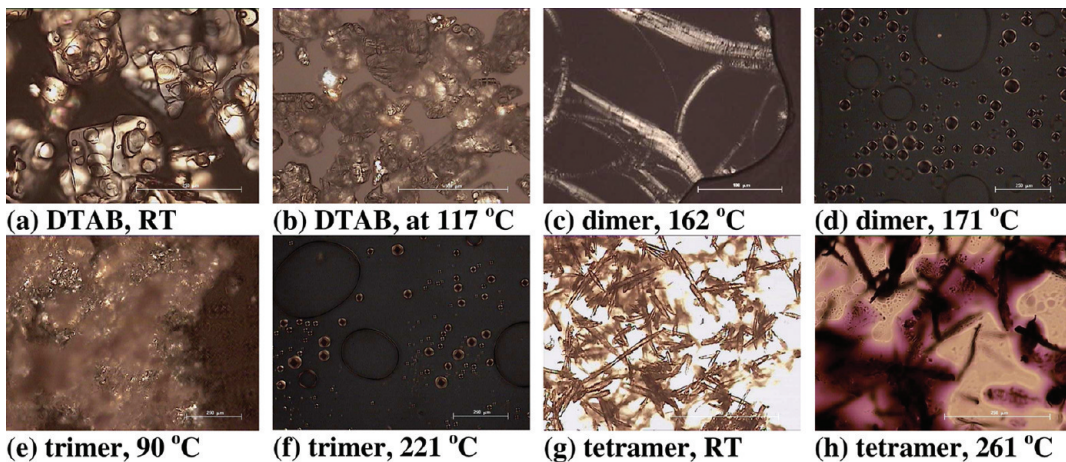


Figure 6. POM microphotographs (the exception is image g, taken without crossed polarizers) of DTAB (a, b), 12-2-12 (c, d), 12-2-12-2-12 (e, f), and 12-2-12-2-12-2-12 (g, h) taken during heating. Temperatures and scale bars are denoted. RT denotes room temperature.

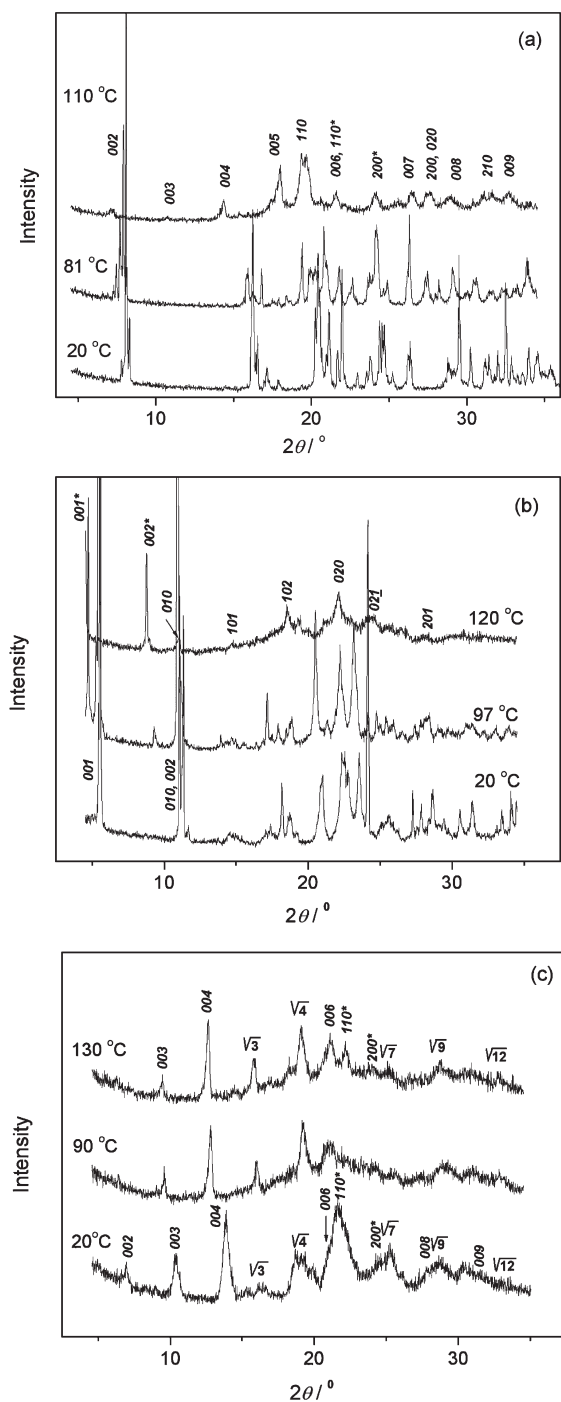


Figure 7. X-ray diffraction patterns of DTAB (a), 12-2-12 (b), and 12-2-12-2-12 (c) taken at different temperatures, as indicated.

first transition resulted in a birefringent phase showing a texture similar to that of the viscous neat phase (Figure 6e). This phenomenon was also reported for gemini surfactants.⁵ Very small changes in two diffractograms taken after the first transition might be ascribed to the formation of varieties of the SC₂ phase (Figure 7c). The persistence of the softened sample with a very high viscosity and birefringent cloudy textures of the SC₂ phases might be ascribed to the SmB phase detected by XRD (Figure 7c). At higher temperatures, the compounds showed a spherulitic-like texture with Maltese crosses (Figure 6f), which is

a characteristic of the SmA phase. Textures were hardly observable because of the very narrow temperature interval of the liquid-crystalline phase appearance and overlapping with the decomposition. In accord with DSC, XRD, and microscopic observations, the sequence of phase transitions may be as follows: SC₁ → SC₂ → SC₂* → LC–IL/decomposition.

The DSC curve for the tetramer showed no transitions inside the solid phase. The exothermic transition at the highest temperatures was associated with the abrupt appearance of black solids (Figure 6h), indicating that extended decomposition preceded melting. The texture observation of the probably formed LC phase was overshadowed because a black solid covered the surface of the sample.

The difference in temperature between melting and decomposition decreases as the degree of oligomerization increases, thus diminishing the range of mesophase stability. This might be ascribed to the strong interactions of quaternary ammonium headgroups with bromide counterions in the solid lattice, contributing to crystal stability and consequently to the increase in the melting point. It is obvious that these interactions are strongest for the tetramer with four quaternary ammonium headgroups, which does not undergo a polymorphic transition in the measured temperature interval and decomposes prior to melting.

The nature of the thermal phase transitions was studied by X-ray powder diffraction. Figure 7a–c represents diffractograms with indexed characteristic reflections for DTAB, the dimer, and the trimer, respectively, all within the solid crystalline region. Diffractograms of melted samples were not taken because of decomposition problems.

Figure 7a shows the diffractograms for DTAB taken at room temperature and after the first and second transitions in the heating cycle. The diffraction pattern at 81 °C (SC₁*) differs only slightly from that taken at room temperature (SC₁), indicating a very small structural change. A slight shift in the main reflections toward lower angles associated with somewhat higher d_{00l} values (22.50 Å), the splitting of the 002 reflection (or the appearance of a new one at $2\theta / {}^\circ = 7.84$), and a small enthalpy change indicate the SC₁* phase as a structural variety. A more expressed shift of mainly 00l diffraction lines (up to the ninth-order reflections (009) in the diffractogram recorded at 110 °C) toward lower angles and the decrease in their relative intensities associated with a significant d_{00l} increase indicate polymorphic transitions to the SC₂ phase. The appearance of a diffuse maximum in the wide-angle region beside 00l reflections is typical of a layered ordering. By utilizing d values of the 00l reflections with the reciprocal spacing ratio 2:3:4, the interlayer distance is 24.60 Å, which corresponds to the interdigitated bilayer. Other reflections in the DTAB diffractogram seem to come from the lateral ordered arrangement of ammonium headgroups and bromide counterions as well as the lateral arrangement of alkyl chains. Relatively strong reflections centered between split peaks 19.52/19.72, 27.2/27.82, and 31.28/31.71 $2\theta / {}^\circ$ are indexed as 110, 200, and 210 reflections of a 2D tetragonal lattice. The splitting of these reflections indicates the transformation of the rectangular base plane of the monoclinic DTAB cell ($a \times b = 5.64 \times 7.26$ Å) with ammonium and bromide ions in a tetragonal form that is somewhat distorted into a rhombic form ($a \times b = 6.37 \times 6.47$ Å). Weaker diffraction lines, centered at 4.08 and 3.68 Å indexed as 110 and 200 reflections (listed in Figure 7a as 110* and 200* as distinct from the 200 peak of lateral ordering of bromide ions), are characteristic of the lateral ordering of *n*-alkyl chains.

They are superimposed on other reflections (110^* to 006 and 200* correspond to the 020 reflection of the lateral stacking of zigzag alkyl chain planes in the monoclinic DTAB cell). Low intensity of the 110^* reflection and the increased intensity of the amorphous halo indicate decreased lateral ordering of the alkyl chains at $110\text{ }^\circ\text{C}$. Obviously, ammonium headgroups and bromide counterions maintain longitudinal smectic and mesomorphic lateral ordering. Crystallization of the sample takes place upon cooling from the melt. Almost the same diffraction patterns of the cooled sample at 97 and $20\text{ }^\circ\text{C}$ (not shown) as obtained for SC_2 and SC_1 phases reveal that polymorphic transitions are reversible. Somewhat broadened reflections with respect to the untreated sample indicate smaller crystals.

Figure 7b shows diffraction patterns of 12-2-12 at room temperature and after the first and second transitions. The diffraction pattern taken after the first transition with most reflections slightly shifted toward smaller angles with decreasing intensities and the appearance of new peaks show the existence of a mixture of SC_1 and SC_2 phases. The most indicative among them is the new peak at a lower diffraction angle, indicating a new higher layer thickness of 18.14 \AA at $97\text{ }^\circ\text{C}$ compared to dimer periodicity at room temperature. It seems that only part of the SC_1 phase was transformed to SC_2 because two endothermic transitions at lower temperatures are closely spaced (Figure 5). The shifting of all $00l$ reflections toward smaller angles indicates an increase in d_{00l} values with increasing temperature (denoted as $00l^*$ reflections in the diffractogram recorded at $120\text{ }^\circ\text{C}$). The diffraction pattern taken after the second transition shows the appearance of two broadened diffuse amorphous maxima in the range of $2\theta/$ from 12 to 35 . These diffuse diffraction maxima indicate the increased disordering of hydrocarbon chains. With respect to room-temperature phase SC_1 , some SC_3 phase maxima (mainly $00l$ reflections) are shifted toward smaller angles and most of the other reflections exhibit diminished intensities or even disappear. The shifting of the $00l$ reflections implies an increase in the d_{00l} values. It seems that the new higher-layer periodicity (19.79 \AA) defined by $00l^*$ reflections replaces the initial layer periodicity (15.48 \AA) defined by $00l$ reflections that almost disappear. Both 001 and 002 reflections are significantly stronger than broadened reflections at medium angles superimposed on the scattered amorphous halo that remains during heating to $120\text{ }^\circ\text{C}$. Other reflections in the diffractogram seem to come from the lateral ordered arrangement of ammonium headgroups and bromide counterions as well as the lateral arrangement of alkyl chains. Residual reflections at medium angles with significantly reduced intensities (peak denoted 020 is most intensive) indicate the arrangement of ammonium headgroups and bromide counterions in polar sublayers.

The existence of two intensive first $00l$ reflections (001 and 002) and a diffuse halo suggests SC_3 as an SmC phase.^{2,16} In an SmC phase, molecules have the same lamellar arrangement as in an SmA phase but the director is tilted toward the plane of a layer. Because alkyl chains are tilted toward the base plane of the unit cell and to c axes in the freshly prepared dimer (Figure 2), their tilting could be possible even at $120\text{ }^\circ\text{C}$. This partially crystalline phase is an intermediate phase between crystalline and liquid-crystalline phases.² All thermal transitions inside SC phases retained the structural ordering of headgroups and counterions to be imposed on the structural disordering of alkyl chains. During transitions at higher temperatures, 12-2-12 adopted a liquid-crystalline structure with textures reminiscent of the SmA phase (Figure 6c,d).

Figure 7c shows diffraction patterns of the freshly prepared trimer sample taken at room temperature and at temperatures after the first and second transitions observed in the DSC curve. The diffractogram taken at room temperature exhibits broadened diffraction maxima superimposed on the diffuse maximum showing characteristics of mesomorphic ordering or very tiny and/or disordered crystallites. Ratios of reciprocal spacings of the first reflections 2:3:4:6 indicate a layered ordering of molecules with periodicity $d_{001} = 25.07\text{ \AA}$. Broadened reflections superimposed on two diffuse maxima originate from diffraction in the lateral mesomorphic arrangement of ammonium headgroups and bromide counterions as well as from the lateral arrangement of alkyl chains. These broadened reflections with a ratio of $(3)^{1/2}:(4)^{1/2}:(7)^{1/2}:(9)^{1/2}:(12)^{1/2}$ for reciprocal spacings indicate the lateral hexagonal arrangement of ammonium headgroups and bromide counterions in polar sublayers, which implies a hexagonal crystal smectic structure. The remaining two peaks were indexed as 110 and 200 reflections (i.e., 110^* and 200^*) of a 2D-centered rectangular lattice. These reflections may indicate the lateral ordering of alkyl chains within the smectic layers. Such a diffractogram may indicate hexagonal lateral ordering with a long-range longitudinal positional order typical of the crystal smectic B phase.

The diffraction pattern at $90\text{ }^\circ\text{C}$ exhibits a significant shift, weakening, and narrowing of $00l$ reflections. Shifts of $00l$ reflections to a lower diffraction angle indicate an increase in layer periodicity from 25.07 to 26.90 \AA . The intensities of 110^* and 200^* reflections, corresponding to the lateral packing of paraffin chains, were remarkably reduced (almost disappeared). Simultaneous increases in the diffuse scattering halo centered at ca. 4.4 \AA indicate the short-range order of disordered alkyl chains. The positions and intensities of reflections with a ratio of $(3)^{1/2}:(4)^{1/2}:(7)^{1/2}:(9)^{1/2}:(12)^{1/2}$ corresponding to the hexagonal lateral packing of ammonium headgroups and bromide counterions remain unchangeable. An exception is the weakening of the $7^{1/2}$ peak, which corresponds to the 200 , 310 , and 320 reflections. Because most of these reflections as well as the $00l$ reflections remain, the longitudinal periodicity of the layers in this mesophase is maintained by the well-defined lateral hexagonal ordering of ammonium headgroups and bromide counterions in polar sublayers. Alkyl chains lose their long-range positional order within layers, indicating a transition to the SmB phase.

The diffraction pattern at $130\text{ }^\circ\text{C}$ differs only slightly from that taken at $90\text{ }^\circ\text{C}$, implying a small difference in structural ordering. A small additional shift of the $00l$ reflections to a lower diffraction angle indicates an additional slight increase in the layer periodicity ($d_{001} = 27.60\text{ \AA}$). Some peaks became narrower and more recognizable, allowing the full resolution of the 006 and 110^* reflections. The weak but observable 110^* reflection indicates the partial ordering of nonseparated interdigitated alkyl chains as sublayers in hydrocarbon interlayers, contributing to the increase in layer periodicity. At the same time, ammonium headgroups and bromide counterions in the polar sublayer maintained their layer periodicity with increased temperature regardless of the transition character.

Most ionic long-chain compounds exhibit a gradual disordering of alkyl chains upon heating (solid-state polymorphism) and a bidimensional disordering of ionic layers upon melting (thermotropic mesomorphism).^{30,31} When a solid undergoes a phase transition by absorbing thermal energy, the transformed phase will possess a higher internal energy. This results in weaker

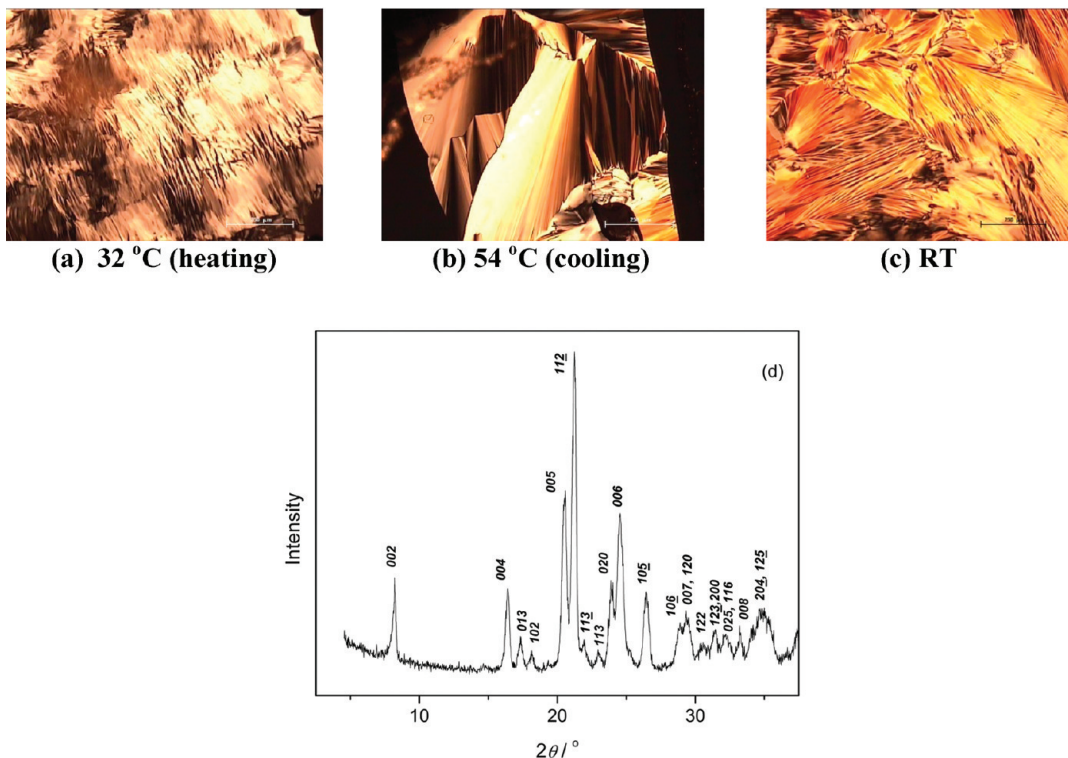


Figure 8. Textures obtained from polarizing microscopy for hydrated DTAB during heating (a) and cooling cycles (b, c). Temperatures and scale bars are indicated. X-ray diffractogram taken at room temperature (RT) upon cooling the hydrated sample (d).

bonding between neighboring atoms or units in the high-temperature phase. Because of the conformational flexibility of the long alkyl chain and weak van der Waals forces between them, more than one type of molecular packing is possible in the solid state, thus allowing the formation of varieties and polymorphs. Because alkyl chains take an ordered arrangement via weak intermolecular forces, the thermal liberation of rotational freedom around the chains takes place at a relatively low temperature. Molecular motion within the chains increases gradually as the temperature increases, until at characteristic temperatures a considerable increase in the molecular motion takes place, causing the formation of various polymorphs. Changes in the diffraction patterns of the DTAB, dimer, and trimer samples with increased temperature revealed polymorphism. Increase in the dodecyl chain number shifted the polymorphic transitions to lower temperatures. In the measured temperature interval, the tetramer exhibited no polymorphic transition.

Thermotropic mesophases, which are regarded as an intermediate state between the crystal and isotropic liquid, include the structural order of polar layers and the structural disorder of nonpolar layers.³¹ DTAB does not form a liquid-crystalline phase, whereas the dimer and trimer form smectic mesophases at increased temperature. The absence of thermotropic phase transitions in the tetramer sample was tentatively attributed to decomposition.

Mesophases of Hydrated Surfactants. Because of thermal instability, it was not possible to melt oligomeric samples fully and subsequently cool them to obtain characteristic textures. Difficulties arising from the thermal decomposition of gemini surfactants have already been discussed in the literature,^{2,5,6} and some authors³² did not even detect thermotropic mesophases. Obstacles to obtaining more information on their thermotropic

mesomorphism may be partially avoided by heating hydrated samples. A drop of water penetrates a sample during heating, and mesophases develop around the anhydrous bulk. This method allows the observation of all successive phases in equilibrium with a high excess of surfactant by increasing the temperature. Samples underwent progressive dissolution via increasing temperature, and mesophases were characterized by their optical textures. Although this method does not provide quantitative information on the composition, observations by polarizing microscopy can give reliable information on phase transitions. Only a few phase diagrams have been reported for DTAB³³ and 12-2-12,² though the trimer and tetramer have not been investigated.

The appearance of DTAB mesophases that occurred by heating and cooling hydrated samples is represented in Figure 8a–c. A fibrous parallel texture (Figure 8a) indicates the existence of a hexagonal phase at lower temperature. The appearance of fan-shaped textures with homeotropic domains implies a transition to the SmA phase at higher temperatures. The results are in accord with literature data showing the rich lyotropic mesomorphism of DTAB as a function of increasing concentration and temperature. Varade et al.³³ have shown that a hexagonal liquid-crystalline phase is stable in concentrated DTAB solutions up to ca. 40 °C, whereas a transition to a lamellar phase occurs above this temperature. The SmA texture showing fan and focal conic textures reappeared first upon cooling from the isotropic phase (Figure 8b). At lower temperatures, this texture disappeared and a fibrous hexagonal phase was observed. Reversible transitions upon heating and cooling are called enantiotropic transitions. Cooled samples showed paramorphism (i.e., the fibrous texture of the previous mesophase was retained) (Figure 8c).

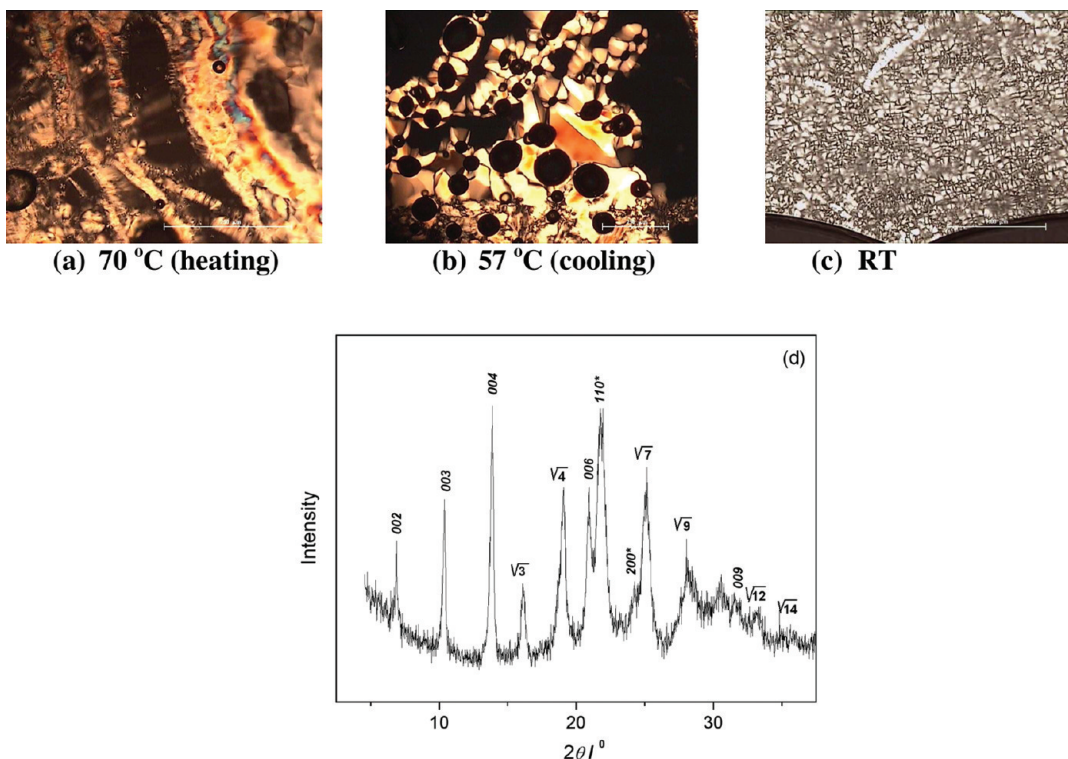


Figure 9. Textures obtained from polarizing microscopy for hydrated 12-2-12 during heating (a) and cooling cycles (b, c). Temperatures and scale bars are denoted. X-ray diffractogram taken at room temperature (RT) upon cooling the hydrated sample (d).

Figure 8d presents the diffractogram of the cooled sample. Concerning angular positions and relative intensities of diffraction lines, this diffraction pattern is almost the same as that of the anhydrous sample taken prior to the heating cycle (Figure 1a). The layer periodicity calculated from $00l$ reflections with a reciprocal Bragg spacing ratio of 2:4:5:6 ($d_{001} = 21.14 \text{ \AA}$) is comparable to the major repeat distance of anhydrous DTAB ($d_{001} = 21.25 \text{ \AA}$).

Upon heating the 12-2-12 sample from room temperature to ca. 70 °C, the coexistence of the two phases was observed: the hexagonal phase identified by fan-shaped patterns and the SmA phase identified by Maltese crosses and oily streaks (Figure 9a). Upon further heating, the hexagonal phase disappeared but the SmA phase persisted. On cooling from the isotropic liquid, the SmA phase reappeared, showing focal conic fan textures with a black area caused by the homeotropic orientation of the molecules. At lower temperature, the texture of the hexagonal phase with a remnant SmA phase persisted close to room temperature (Figure 9b), suggesting the slow process of transformation. The sample aged for 2 weeks at room temperature retained the mosaic texture showing paramorphism (Figure 9c). The diffraction pattern taken at room temperature displays the characteristic peaks of a virgin crystal; however, the presence of a small amount of an amorphous phase indicates that crystallization is kinetically controlled. The interlayer spacing upon cooling to the room-temperature phase is 14.95 Å, which is somewhat smaller than that of the virgin sample.

POM images of 12-2-12-2-12 obtained by heating and cooling are presented in Figure 10a–c. The mesophase in the heating mode was a hexagonal phase (Figure 10a). The hexagonal phase reappeared upon cooling and persisted down to ca. 66 °C. Upon further cooling, the mosaic platelet texture

(Figure 10b) was observed down to ca. 36 °C. This kind of texture is often observed for highly ordered smectic phases. At room temperature, the sample exhibited a texture resembling the crystal smectic B phase (Figure 10c).²⁴

The diffraction pattern of the 12-2-12-2-12 sample cooled to room temperature (Figure 10d) similar to that of the fresh anhydrous sample taken prior to the heating cycle indicates a crystal smectic B phase. However, more intensive, sharper, and resolved reflections in the diffractogram of the cooled sample indicate better hexagonal ordering compared to the diffractogram of the freshly prepared anhydrous sample (Figure 7c). It seems that molecular mobility enhanced by heating and slow cooling of the hydrated sample contributes to an advanced ordering. The layer periodicity ($d_{001} = 25.14 \text{ \AA}$, calculated from $00L$ reflections) is similar to that for the aged sample ($d_{001} = 25.07 \text{ \AA}$). More than two $00l$ reflections and the reflections at medium angles with the $(3)^{1/2}:(4)^{1/2}:(7)^{1/2}:(9)^{1/2}:(12)^{1/2}$ ratio of reciprocal interplanar spacings indicate a highly ordered crystal smectic B phase. However, significantly more expressive and resolved reflections of the cooled hydrated sample (Figure 10d) than in the anhydrous freshly prepared sample could be ascribed to better interlayer stacking. Namely, the crystal smectic B phase can show some variations in the interlayer stacking, and mono-, bi-, and trilayer unit cells can be obtained.¹⁶

At room temperature, hydrated 12-2-12-2-12-2-12 showed lancetlike textures that might be ascribed to the viscous SmT phase.²⁴ On heating, transition to textures typical of the hexagonal phase occurred (Figure 11a). The hexagonal phase reappeared on cooling and persisted down to ca. 41 °C. On further cooling, a mixture with the remnant hexagonal phase and Schlieren textures was observed (Figure 11b). Both textures disappeared on cooling to room temperature, and after a few

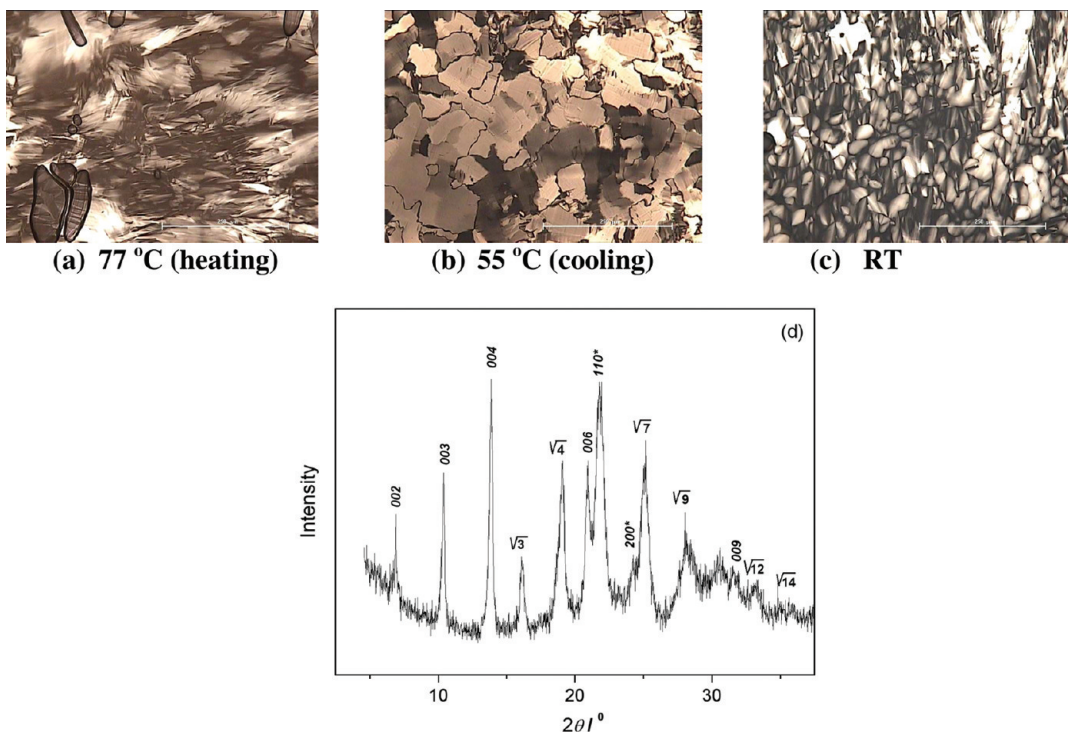


Figure 10. Textures obtained from polarizing microscopy for hydrated 12-2-12-2-12 during heating (a) and cooling cycles (b, c). Temperatures and scale bars are denoted. X-ray diffractogram taken at room temperature (RT) upon cooling of the hydrated sample (d).

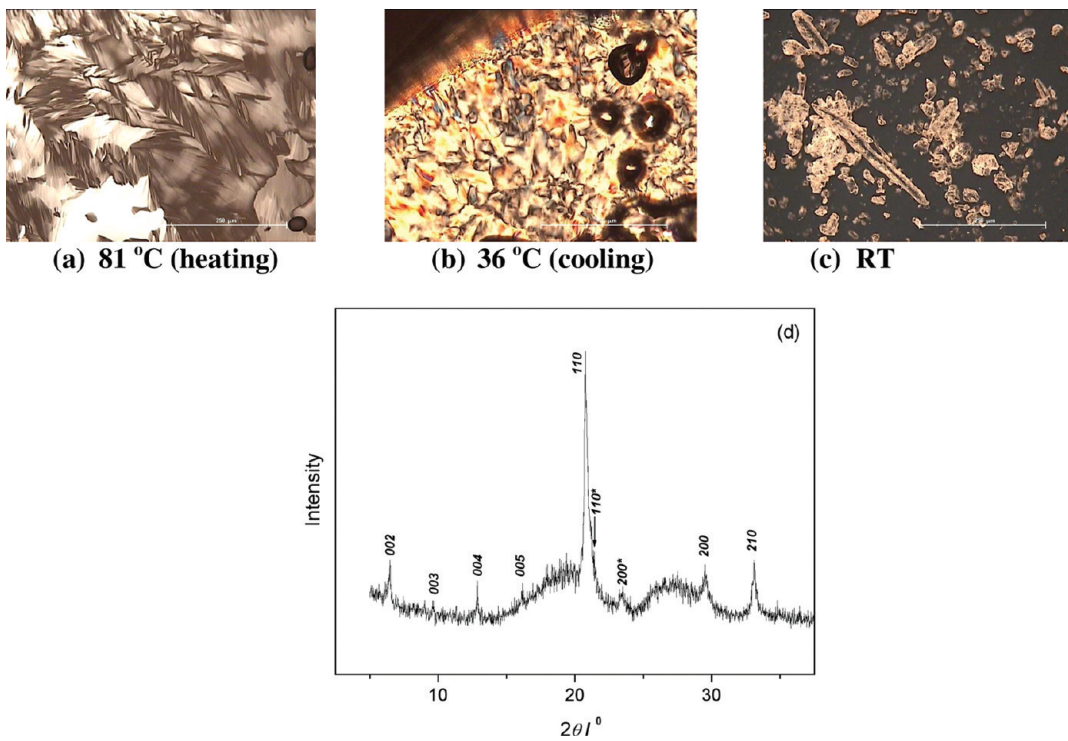


Figure 11. Textures obtained from polarizing microscopy for hydrated 12-2-12-2-12-2-12 during heating (a) and cooling cycles (b, c). Temperatures and scale bars are denoted. X-ray diffractogram taken at room temperature (RT) upon cooling of the hydrated sample (d).

hours, anisotropic lancetlike crystals and agglomerates of smaller crystals were observed (Figure 11c). This might be ascribed to the texture of the crystal smectic T phase.

The diffraction pattern of the 12-2-12-2-12-2-12 sample cooled to room temperature (Figure 11d) was similar to that of the anhydrous sample taken prior to the heating cycle. The

ratio of reciprocal spacing values 2:3:4:5 indicates layered ordering with the same interplanar spacing ($d_{001} = 27.27 \text{ \AA}$) as for the virgin sample ($d_{001} = 27.25 \text{ \AA}$). The $00l$ reflections are weaker than those for the virgin sample; some of them (008, 009, 0010) even disappeared. As in the virgin sample, expressed reflections denoted as 110, 200, and 210 arose from the mesomorphic tetragonal ordering of headgroups and the counterion layer. Unit cell parameter a of the square lattice is the same as in the virgin sample ($a = 6.04 \text{ \AA}$). Also, the 110 and 200 reflections, centered at ca. 4.16 and 3.78 \AA could be indexed as those of a 2D-centered rectangular lattice (i.e., 110* and 200*) corresponding to the lateral ordering of alkyl chains within the smectic layers. The diffractogram of the cooled tetramer also exhibits the same diffuse diffraction halos as the virgin sample.

The manner in which surfactant molecules are arranged in the solid phase correlates with their solution behavior (i.e., there is a strong relationship among the structure of surfactant molecules, the crystal structure, and the type and structure of supramolecules self-assembled in aqueous solutions). The formation of lyotropic mesophases depends on the surfactant concentration and the degree of curvature determined by the packing arrangements of amphiphilic molecules. These factors correlate with the equilibrium area per surfactant headgroup at the air/solution interface, which directly affects the preferred morphology of a supramolecule.³⁴ For example, the small surface area occupied by one headgroup at the interface causes a low curvature phase and vice versa. In the low curvature lamellar phase, the constituent molecules are arranged in layers. Increased curvature produces a hexagonal phase where the surfactant molecules form a columnar structure that can be packed in hexagonal arrays; further increasing the curvature results in the formation of micelles. The sequence of lyotropic mesophases of hydrated surfactants upon increasing the temperature within the oligomeric surfactant series is in accord with the general observation. With increasing temperature, hydrated dimer and monomeric counterpart samples displayed a sequence of phases typical of concentrated surfactant systems comprising a hexagonal phase at lower temperatures and a smectic phase at higher temperatures. On the contrary, the trimer and tetramer displayed upon heating only textures of hexagonal phases. This may be attributed to the increase in the surface area occupied by headgroups at the interface,¹⁴ which favors structures of higher curvature.

In terms of the oligomeric surfactant structure, one can expect that a more highly charged headgroup will tend to delay the formation of less-curved phases. A short ethylene spacer lying flat at the oligomeric surfactant supramolecule/solution interface holds quaternary ammonium headgroups closer to each other in contrast to the equilibrium distance determined by the opposite forces at play in supramolecule formation (i.e., the headgroup distance distribution is bimodal).

CONCLUSIONS

A series of cationic oligomeric surfactants (quaternary dodecyldimethylammonium ions with two, three, or four chains connected by an ethylene spacer at the headgroup level) were synthesized and characterized. Their structural properties, polymorphism, and mesomorphism were investigated by various complementary methods.

Diffractograms of DTAB and the dimer with a number of sharp Bragg reflections without amorphous halos show the existence of fully crystalline samples with well-developed 3D

ordering. In contrast, diffraction patterns of the trimer and tetramer reveal the existence of less-ordered solid phases (i.e., their XRD patterns are typical of highly ordered crystal smectic B and T phases, respectively). All diffractograms show small-angle reflections with reciprocal spacing in the ratio 1:2:3:4, indicating that the molecules form layers. The major interlayer distance increased from dimer to tetramer; however, all d values significantly smaller than the double extended dodecyl chain indicated chain interdigitation.

All anhydrous compounds exhibit complex thermal behavior characterized by several successive phase transitions in the solid state. On heating, oligomers and their monomeric counterpart display phase transitions in several steps. Transitions between various structural forms occur at definite temperatures and are accompanied by the exchange of latent heat, which depends on the chain number. The number of thermal phase transitions and sequence of phases are markedly affected by the number of dodecyl chains whereas the monomeric counterpart exhibits only polymorphism and the dimeric and trimeric surfactants exhibit complex polymorphism and thermotropic mesomorphism from the solid to the liquid-crystalline phases of the smectic type. In contrast, the tetrameric surfactant displays only transitions at higher temperature associated with decomposition covering the possible liquid-crystalline phase transitions. As the number of chains increases, the temperature difference between melting and maximum decomposition decreases, thus diminishing the range of mesophase stability. This is ascribed to the increase in the melting point due to strong electrostatic interactions of quaternary ammonium headgroups with bromide counterions in the solid lattice.

Changes in the diffraction patterns of the DTAB, dimer, and trimer samples with the change in temperature indicate rearrangements in the crystal lattice and mesostructural transitions. Transitions through polymorphic states are in accord with the transitions observed in DSC curves. A constant decrease in intensity of some reflections or even the disappearance of peaks due to the hydrocarbon chain (200 and 110) with a simultaneous increase in the amorphous halo assigned to frozen hydrocarbon chains indicates a diminished ordering of the alkyl chains in layers.

Hydrated samples exhibit lyotropic mesomorphism by showing reversible phase transitions on heating and cooling that are typical of concentrated ionic surfactant systems. The sequence of liquid-crystalline phases for DTAB and dimers is hexagonal at lower temperatures and smectic A at higher temperatures. On heating, both the trimer and tetramer display textures of the hexagonal phase.

ASSOCIATED CONTENT

S Supporting Information. POM microphotographs of 12-2-12 and 12-2-12-2-12 at room temperature. DSC cooling curves of DTAB and 12-2-12. This material is available free of charge via the Internet at <http://pubs.acs.org>.

AUTHOR INFORMATION

Corresponding Author

*E-mail: djurasin@irb.hr.

ACKNOWLEDGMENT

This work was supported by the Ministry of Science, Education and Sports of the Republic of Croatia (grants 098-0982915-2949, 098-0982904-2955, and 098-0982915-2948).

■ REFERENCES

- (1) Zana, R. Dimeric and Oligomeric Surfactants. Behavior at Interfaces and in Aqueous Solution: A Review. *Adv. Colloid Interface Sci.* **2002**, *97*, 205–253.
- (2) In, M.; Zana, R. Phase Behavior of Gemini Surfactants. *J. Disp. Sci. Technol.* **2007**, *28*, 143–154.
- (3) Laschewsky, A.; Wattebled, R.; Arotcarena, M.; Habib-Jiwan, J.-L.; Rakotoaly, R. H. Synthesis and Properties of Cationic Oligomeric Surfactants. *Langmuir* **2005**, *21*, 7170–7179.
- (4) Wattebled, L.; Laschewsky, R.; Moussa, A.; Habib-Jiwan, J.-L. Aggregation Numbers of Cationic Oligomeric Surfactants: A Time-Resolved Fluorescence Quenching Study. *Langmuir* **2006**, *22*, 2551–2557.
- (5) Fuller, S.; Shinde, N. N.; Tiddy, G. J. T. Thermotropic and Lyotropic Mesophase Behavior of Amphitropic Diammonium Surfactants. *Langmuir* **1996**, *12*, 1117–1123.
- (6) Dreja, M.; Gramberg, S.; Tieke, B. Cationic Amphitropic Gemini Surfactants with Hydrophylic Oligo(oxyethylene) Spacer Chains. *Chem. Commun.* **1998**, *1371*–1372.
- (7) Hattori, N.; Masuda, H.; Okabayashi, H.; O'Connor, C. J. Crystal Structures Bis(Quaternary Ammonium Bromide) Surfactants, Ethane-diy-1,2-bis(Butyldimethylammonium Bromide) Dihydrate and Propa-nediy-1,3-(Butyldimethylammonium Bromide). *J. Mol. Struct.* **1998**, *471*, 13–18.
- (8) Sikirić, M.; Šmit, I.; Tušek-Božić, Lj.; Tomašić, V.; Pucić, I.; Primožič, I.; Filipović-Vinceković, N. Effect of the Spacer Length on the Solid Phase Transitions of Dissymmetric Gemini Surfactants. *Langmuir* **2003**, *19*, 1044–10053.
- (9) Caracciolo, G.; Mancini, G.; Bombelli, C.; Cmimiti, R. The Structure of Gemini Surfactant Self-Assemblies Investigated by Energy Dispersive X-ray Diffraction. *Chem. Phys. Lett.* **2004**, *386*, 76–82.
- (10) Wang, Y.; Marques, E. F. Thermotropic Phase Behavior of Cationic Gemini Surfactants and their Equicharge Mixtures with Sodium Dodecyl Sulfate. *J. Phys. Chem. B* **2006**, *110*, 1151–1157.
- (11) Zhou, T.; Zhao, J. Synthesis and Thermotropic Liquid Crystalline Properties of Heterogemini Surfactants Containing a Quaternary Ammonium and a Hydroxyl Group. *J. Colloid Interface Sci.* **2009**, *331*, 476–483.
- (12) Bara, J. E.; Hatakeyama, E. S.; Wiesenauer, B. R.; Zeng, X.; Noble, R. D.; Gina, D. L. Thermotropic Liquid Crystal Smectic Behaviour of Gemini Imidazolium-Based Ionic Amphiphiles. *Liq. Cryst.* **2010**, *37*, 1587–1599.
- (13) Wei, Z.; Wei, X.; Sun, D.; Liu, J.; Tang, X. Crystalline Structures and Mesomorphic Properties of Gemini Diammonium Surfactants with a Pendant Hydroxyl Group. *J. Colloid Interface Sci.* **2011**, *354*, 677–685.
- (14) Jurašin, D.; Habuš, I.; Filipović-Vinceković, N. Role of the Alkyl Chain Number and Head Groups Location on Surfactants Self-Assembly in Aqueous Solutions. *Colloids Surf., A* **2010**, *368*, 119–128.
- (15) Imam, T.; Devinsky, F.; Lacko, I.; Mlynarčík, D.; Krasnec, L. Preparation and Antimicrobial Activity of Some New Bisquaternary Ammonium Salts. *Pharmazie* **1983**, *38*, 308–310.
- (16) Demus, D., Goodby, J., Gray, G. W., Spiess, H.-W., Vill, V., Eds.; *Handbook of Liquid Crystals*; Wiley-VCH: Weinheim, Germany, 1998; Vol. I.
- (17) Bragg, W. L. *Proc. Cambridge Philos. Soc.* **1913**, *17*, 43–57.
- (18) Kamitori, S.; Sumimoto, Y.; Vongbupnimit, K.; Noguchi, K. Molecular and Crystal Structures of Dodecytrimethylammonium Bromide and its Complex with p-Phenylphenol. *Mol. Cryst. Liq. Cryst. Sci. Technol., Sect. A* **1999**, *300*, 31–43.
- (19) Berthier, D.; Buffeteau, T.; Leger, J.-M.; Oda, R.; Huc, I. From Chiral Counterions Twisted Membranes. *J. Am. Chem. Soc.* **2002**, *124*, 13486–13494.
- (20) Tanford, C. *The Hydrophobic Effect: Formation of Micelles and Biological Membranes*, 2nd ed.; Wiley: New York, 1980; pp 74–75.
- (21) (a) Pauling, L. *The Nature of the Chemical Bond*, 3rd ed.; Cornell University Press: New York, 1980; Chapter 1. (b) Dean, J. A. *Lange's Handbook of Chemistry*; McGraw-Hill: New York, 1993; pp 1–5.
- (22) Binnemans, K. Ionic Liquid Crystals. *Chem. Rev.* **2005**, *105*, 4148–4204.
- (23) Axenov, K. V.; Laschat, S. Thermotropic Ionic Liquid Crystals. *Materials* **2011**, *4*, 206–259.
- (24) Alami, E.; Levy, H.; Zana, R.; Weber, P.; Skoulios, A. A New Smectic Mesophase with Two Dimensional Tetragonal Symmetry from Dilykdimethylammonium Bromides: S_T . *Liq. Cryst.* **1993**, *13*, 201–212.
- (25) Goossens, K.; Lava, K.; Nocckemann, P.; Van Hecke, P.; Van Meervelt, L.; Driesen, K.; Görller-Walrand, C.; Binnemans, K.; Cardinales, T. Pyrrolidinium Ionic Liquid Crystals. *Chem.—Eur. J.* **2009**, *15*, 656–674.
- (26) Luzzati, V. X-ray Diffraction Studies of Lipid–Water Systems. In *Biological Membranes: Physical Fact and Function*; Chapman, D., Ed.; Academic Press: London, 1968; pp 71–123.
- (27) Jana, T.; Nandi, A. K. Sulfonic Acid-Doped Thermoreversible Polyaniline Gels: Morphological, Structural, and Thermodynamical Investigations. *Langmuir* **2000**, *16*, 3141–3147.
- (28) Jana, T.; Chatterjee, J.; Nandi, A. K. Sulfonic Acid Doped Thermoreversible Polyaniline Gels. 3. Structural Investigations. *Langmuir* **2002**, *18*, 5720–5727.
- (29) Iwamoto, K.; Ohnuki, Y.; Sawada, K.; Seno, M. Solid-Solid Phase Transitions of Long-Chain n-Alkylammonium Halides. *Mol. Cryst. Liq. Cryst.* **1981**, *73*, 95–103.
- (30) Filipović-Vinceković, N.; Pucić, I.; Popović, S.; Tomasić, V.; Težak, Đ. Solid Phase Transitions of Catanionic Surfactants. *J. Colloid Interface Sci.* **1999**, *188*, 396–403.
- (31) Busico, V.; Ferraro, A.; Vacatello, M. Thermotropic Smectic Liquid Crystals of Ionic Amphiphilic Compounds: A General Discussion. *Mol. Cryst. Liq. Cryst.* **1985**, *128*, 243–261.
- (32) Alami, E.; Levy, H.; Zana, R. Alkanediyl- α,ω -bis(Dimethylalkylammonium Bromide) Surfactants. 2. Structure of the Lyotropic Mesophases in the Presence of Water. *Langmuir* **1993**, *9*, 940–944.
- (33) Varade, D.; Aramaki, K.; Stubenrauch, C. Phase Diagrams of Water–Alkyltrimethylammonium Bromide Systems. *Colloids Surf., A* **2008**, *315*, 205–209.
- (34) Israelachvili, J. N. *Intermolecular and Surface Forces*; Academic Press: London, 1992; Chapter 17.